

## BARITE NODULES IN PERMIAN KARST SEDIMENTS OF THE NORTHERN GREYWACKE ZONE NEAR KITZBÜHEL (TYROL, AUSTRIA)

Karl Krainer

With 7 figures, 2 tables and 4 plates

### Abstract:

Spherical to subspherical barite nodules are a common constituent in Lower Permian karst sediments of the Devonian Spielberg Dolomite of the Northern Greywacke Zone near Kitzbühel (Austria). The barite nodules are up to several centimeters in size and composed of large, lath like, randomly oriented, inclusion-pure barite crystals and a thin rim of authigenic quartz, dolomite and mica.

It is assumed that the barite nodules are of early diagenetic origin and that originally they were composed of fine-grained barite intergrown with interstitial clay minerals. The unusual mineralogical composition and texture of the nodules were caused by a late diagenetic and particularly an early Alpine very low grade metamorphic overprint. The source of the Ba is unknown; it was probably remobilized from older rocks.

### Zusammenfassung:

In unterpermischen Karstsedimenten des devonischen Spielbergdolomites (Nördliche Grauwackenzone) treten in der Nähe von Kitzbühel häufig rundliche Barytkonkretionen auf. Die Barytkonkretionen werden bis zu mehrere Zentimeter groß und bestehen aus großen, leistenförmigen, nicht orientierten, reinen Barytkristallen und einem dünnen Saum aus Quarz, Dolomit und neu gesprossenen Hellglimmern.

Die Barytkonkretionen entstanden vermutlich frühdiagenetisch durch Ausfällung aus Ba-reichen Porenwässern und waren ursprünglich wohl aus feinkörnigem Baryt mit tonigen Verunreinigungen zusammengesetzt. Die ungewöhnliche Struktur und Zusammensetzung der Konkretionen wird auf eine spätdiagenetische Überprägung und vor allem auf eine sehr schwache, frühalpidische Metamorphose zurückgeführt. Die Herkunft des Ba ist nicht bekannt, vermutlich wurde das Ba aus älteren Gesteinen remobilisiert.

### 1. Introduction

Barite nodules of diagenetic origin have been described from sediments of different environmental settings. They seem to occur most frequently in pelagic sediments, particularly of Paleozoic (Silurian, Devonian and Early Carboniferous) age, but are also known from red beds and even from lacustrine deposits and coal seams. Barite nodules from pelagic sediments are described for example by BOGOCH et al. (1977), CLARK (1985), CLARK & MOSIER (1989), HOLDEN (1977), CARLSON & HOLDEN (1979), NUELLE & SHELTON (1986), LAZNICKA (1976), PEPPER et al. (1985), WETZEL (1970) and ZIMMERMANN & AMSTUTZ (1966). Examples of barite nodules in

red beds are reported by VAN EEDEN (1937), HAM & MERRITT (1944), KEYSER (1966) SHEAD (1923) and TARR (1933), for example. HEMINGWAY & VONDRA (1992) reported barite nodules from Lower Cretaceous lacustrine sediments of Wyoming. Concretionary barite also occurs in Eocene brown coal seams of the Geiseltal (HAAGE & KRUMBIEGEL, 1968). Barite nodules are also known from modern ocean floor sediments (REVELLE & EMERY, 1951).

In this paper the term "nodule" is used as a general term which includes concretions as well as rosettes, which have radiating structures. To the author's knowledge, barite has not yet been reported from (paleo-) karst systems. The barite occurrences described in this study are

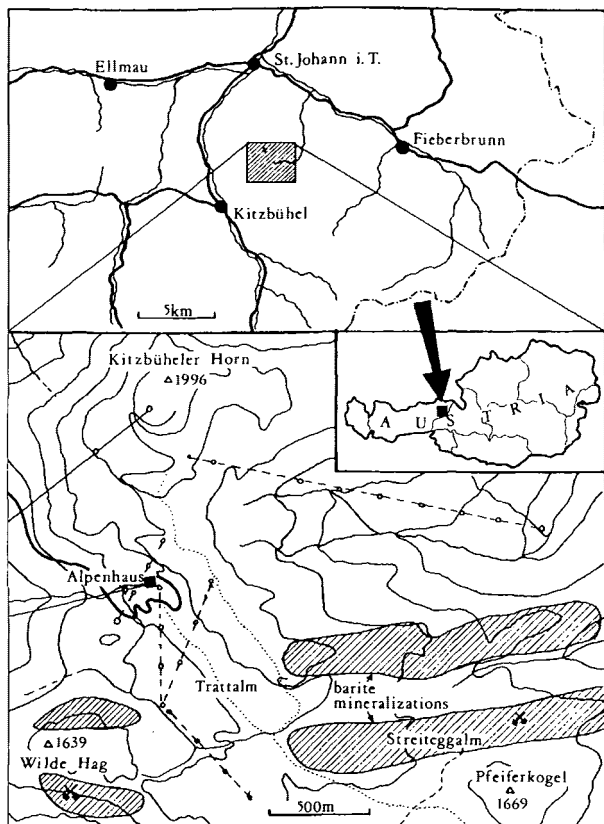


Fig. 1: Location map of the investigated area. Barite mineralization (indicated by hatch pattern) occurs at the localities Wilde Hag and Streiteggalm.

clearly associated with Permian paleokarst features and therefore appear to represent a new, hitherto unrecognized type of syndimentary to early diagenetic barite formation.

The objectives of this study are to give a brief sedimentological description of the host sediments, to characterize the barite nodules in terms of their mineralogical composition and texture, and to discuss the formation of these nodules.

## 2. Location and Geological Setting

The locality of the Permian karst sediments containing barite concretions is situated in the Kitzbühel Alps near the town of Kitzbühel, about 1 km south and southeast of the Kitzbüheler Horn (1996 m) (localities “Wilde Hag” and “Streiteggalm”; see fig. 1). The rocks exposed in

this area are part of the Northern Greywacke Zone, an Upper Austroalpine tectonic unit, and belong to the “Tectonic Unit II” according to MAVRIDIS & MOSTLER (1970).

Stratigraphically the Northern Greywacke Zone comprises Ordovician to Early Silurian Wildschönau Slates (Wildschönauer Schiefer) and intercalated volcanic rocks (porphyroids), Silurian cherts and dark dolomites and dolostones of Devonian age (Spielberg Dolomite). The latter is a light grey coloured, massive to indistinctly bedded bioclastic carbonate sediment, dated as Early to Middle Devonian (Emsian-Eifelian) (EMMANUILIDIS & MOSTLER, 1970, MAVRIDIS & MOSTLER, 1970, MOSTLER, 1970).

The Spielberg Dolomite underwent intense karstification during the Late Carboniferous/Early Permian. Karst fissures and cavities are filled with fine-grained, red karst sediments and barite (figs. 3 and 4). Both, Spielberg Dolomite and karst sediments, are overlain by a thick sequence of Permian red beds (Basalbreccia, Spielbach shales, Spielberg conglomerate and Mühlbach shales) summarized as “Prebichlschichten” by STINGL (1983).

At the locality “Wilde Hag”, the Early Permian Basalbreccia is 30–40 m thick and composed of dolomite clasts derived from the underlying Spielberg Dolomite, embedded in a shaly to sandy, red-coloured groundmass.

At the locality “Streiteggalm” the Basalbreccia and younger sediments have been eroded (see fig. 2).

The rocks of the studied area have experienced low-grade Alpine metamorphism. The formation of stilpnomelane, phengitic muscovite, chlorite, actinolite and epidote in magmatic rocks, the occurrence of chloritoid, pyrophyllite and mixed-layer paragonite-muscovite in the Wildschönau Slates and the lack of prehnite, pumpellyite and lawsonite indicate lower greenschist facies with temperatures of 350–400°C and pressures of 3–8 kb (HOSCHEK et al., 1980, COLLINS et al., 1980, SCHRAMM, 1980). “Illite crystallinity” (IC) data are consistent with these results. IC values decrease systematically from S to N, indicating decreasing intensity of meta-

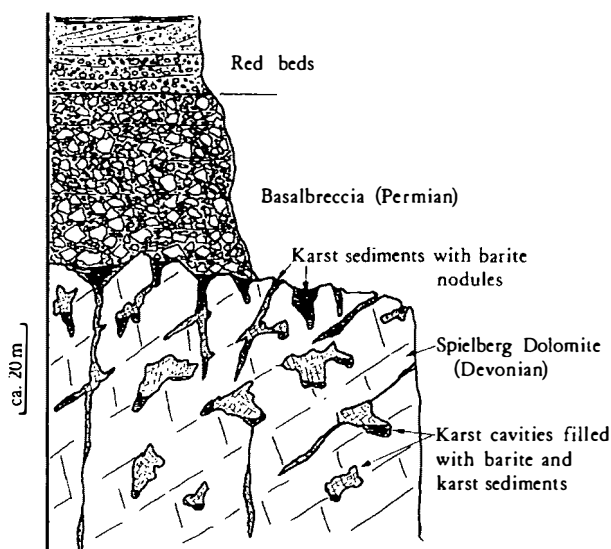


**Fig. 2:** Generalized section of the karstified Spielberg Dolomite (Devonian) and the overlying Lower Permian red beds (basalbreccia, conglomerates, sandstones).

morphism in this direction (SCHRAMM, 1977, 1978, 1980). K-Ar and Rb-Sr ages of illite range from 137 to 92 Ma and indicate an Early Cretaceous metamorphic overprint (KRÁLIK et al., 1987).

### 3. Methods of investigation

Compositional and textural parameters of the karst sediments and barite nodules were investigated by thin section microscopy.

Chemical analyses of mineral phases (detrital micas, micas of the concretions, dolomite) were performed using an electron microprobe (ARL-SEM-Q). Operating conditions for wavelength-dispersive analysis were 15 kV accelerating voltage, 20  $\mu$ A sample current and 200  $\mu$ A emission current.

The Sr content of the barite was measured by X-ray fluorescence analysis. Cathodoluminescence (CL) microscopy was performed using a Technosyn cold-cathode luminoscope.

## 4. Karst sediments and barite nodules

### 4.1 Sedimentology of the karst sediments

In the Northern Greywacke Zone Late Paleozoic karstification features are widespread and occur in Devonian dolomites of the western part (Spielberg Dolomite, Schwaz Dolomite) as well as in the eastern part (MOSTLER, 1984, STINGL, 1983, KRÄINER & STINGL, 1986). Lower Carboniferous paleokarst has recently been described from Devonian to Lower Carboniferous limestones of the Carnic Alps (SCHÖNLAUB et al., 1991).

Two events of karstification can be recognized according to MOSTLER (1984):

- a Variscan event during the Viséan, and
- a late- to post-Variscan event during the Late Carboniferous and Early Permian.

Mineralizations of barite, fahlore, magnesite and siderite are associated with these paleokarst features.

The surface of the Spielberg Dolomite is characterized by a marked karst topography with karst fissures (joints extended by karst dissolution) and irregular cavities extending more than 150 m beneath the surface of the Spielberg Dolomite.

Karst fissures and cavities are filled with different types of sediment and with barite (figs. 3 and 4). Red, fine-grained sediments are most abundant.

The red karst sediments are mostly massive to indistinctly laminated; locally the sediment is well-laminated due to sudden changes in grain size or composition (carbonate-quartz-mica content).

In a few samples erosional surfaces filled by coarser, quartz-rich sediments, have been observed under the microscope.

The karst sediments are moderately to poorly sorted. Detrital grains including quartz grains are angular. The original rounding of the dolomite rhombs is diagenetically overprinted. Micas and elongated quartz grains are commonly oriented parallel to the bedding plane.



Fig. 3: Karst cavities within the Devonian Spielberg Dolomite at the locality Streitegg Alm, filled by red karst sediment and barite. Pencil for scale.



Fig. 4: Irregular karst cavities from the deeper part of the Permian karst system within the Spielberg Dolomite. The cavities are almost completely filled by barite. Pocket lamp for scale.

In most samples grain size ranges from 0.03–0.07 mm (coarse silt), in coarser laminae from 0.1–0.15 mm (fine sand). Some detrital quartz and mica grains may be up to 0.5 mm in diameter (medium sand).

The dolomite content of the red karst sediments in some samples exceeds 80%. In some layers detrital quartz is the most frequent grain type and occurs in form of monocrystalline, elongated fragments. Detrital micas, which are dominated by muscovite and degraded bitotites are abundant in some samples. Some micas are bent or broken due to mechanical compaction. Diagenetically formed hematite is dispersed in the groundmass and concentrated along cleavage planes of biotite grains. Hematite is also found as euhedral crystals locally forming rosettes.

In most samples matrix content is high and consists of carbonate cement and clay (e.g. in quartz- and mica-rich sediments). Some quartz cement (authigenic overgrowths) is also present.

A variety of sediments occurs within paleo-karst dissolution cavities, including carbonates, sandstones, siltstones and shales:

- a) Fine-grained, red to brownish dolomite with variable clay content (pl. 1, fig. 4). The dolomite grains (about 0.05 mm in diameter) are anhedral to euhedral, recrystallized and frequently zoned with inclusion-rich cores and clear rims. The dolomite rhombs are also zoned under cathodoluminescence with bright yellowish-red cores and dull rims, suggesting that the rims contain more Fe than the cores. In some samples the boundary between core and rim is gradual. Some dolomite rhombs are characterized by dull luminescent cores. The clay-rich groundmass between the dolomite rhombs is composed of illite-sericite, and minor hematite. Detrital micas and angular quartz grains may also occur. Some samples from the “Wilde Hag” contain rock fragments of red shales, fine-grained sandstones, polycrystalline quartz of metamorphic origin and phyllitic grains with diameters up to several mm. Accessory constituents are tourmaline and zircon.



- b) Red shales composed of illite-sericite and hematite, with few dolomite rhombs (up to 0.3 mm), detrital micas and angular quartz grains (up to 0.15 mm: mostly monocrystalline quartz) and muscovite-sericite (pl. 1, fig. 5; pl. 3, fig. 3). Detrital feldspars are absent.
- c) Several mm thick, fine-grained sandstone layers (mostly 0.1–0.2, max. 0.5 mm) containing angular quartz (mostly monocrystalline quartz), muscovite-sericite, some biotite and accessory grains of brownish tourmaline and zircon (pl. 3, fig. 5).
- d) Karst breccias (rare) composed of densely packed angular clasts of Spielberg Dolomite embedded in an argillaceous red groundmass. Karst breccias formed at the base of cavities and are overlain by fine-grained dolomitic sediments.
- e) Thin hematite crusts are locally observed within fine-grained karst sediments, indicating periods of non-deposition.

#### 4.2 Barite nodules

The karst sediments are characterized by different types of barite mineralization. Karst cavities may be completely filled by barite, particularly in the deeper parts of the karst system (fig. 4), or barite occurs within the karst sediments as irregular, non-stratabound mineralizations and concretions (fig. 3) (MOSTLER, 1970, MOSTLER et al., 1982).

Individual bodies of barite are up to 2 m thick. The coarse-grained barite of the karst cavities has been mined in the last century.

At the locality Streiteggalm barite concretions are a common constituent of the fine-grained, red-coloured karst sediments (figs. 5, 6, 7). Barite concretions are less common in karst sediments at the locality Wilde Hag.

The occurrence of barite concretions at these localities has first been reported by LEITMEIER (1936) and VOHRYZKA (1968), who described them as "Barytkugeln".

The largest barite concretions with diameters up to 20 cm have been found at the Wilde Hag.



**Fig. 5:** Small karst cavity filled by red karst sediment, locality Streitegg Alm. A barite nodule composed of white, lath like barite crystals occurs within the karst sediment.



**Fig. 6:** A several cm large elongated nodule composed of coarse, lath-like barite crystals embedded in fine-grained red karst sediments (Streitegg Alm).

whereas at the Streiteggalm the size of the concretions varies between 0.2 cm and a few centimeters. The shape of the concretions is spherical to oval with the larger diameter parallel to the bedding plane. The color of the barite concretions is uniformly white.

Three different types of concretions can be distinguished based on the size and mineralogical composition: dolomite concretions (<1 mm), barite-dolomite concretions (1–5 mm) and almost pure barite concretions (> 5 mm).

### a) Dolomite concretions

These concretions generally do not show a distinct separation into core and rim, although quartz is more abundant at the margin and micas are concentrated in the center (pl. 2, fig. 2). They are composed of authigenic minerals, particularly dolomite, and smaller amounts of quartz and mica. Two phases of dolomite have been recognized: dolomite I replaced by quartz, and dolomite II which is replacing quartz. Toward the margin of the concretions the mica content and the grain size decrease. In the center of the concretions mica crystals display a radial arrangement, individual mica crystals are up to 0.8 mm in length (pl. 3, fig. 4). Quartz is polycrystalline with different grain sizes, smaller at the margins, with increasing grain size toward the center. Dolomite occurs as euhedral rhombs at the margin and as irregular patches in the center, replacing quartz. Micas are intergrown with dolomite and quartz and replaced them.

In one sample several smaller concretions (0.5–0.8 mm) composed of a dolomitic core and a quartz rim have been observed. Quartz crystals show general increase in size from the rim to the core of the concretion. Quartz replaces dolomite



**Fig. 7:** Red karst sediment (siltstone) with abundant small barite concretions. Polished slab, Streitegg Alm.

in this sample. A few dolomite rhombs and small mica flakes are also present within the quartz-rich rim.

### **b) Dolomite-barite concretions**

Dolomite-barite concretions are intermediate in size (1–5 mm) and composed of a barite core and an outer zone of dolomite (pl. 2, fig. 2). The core consists of one or a few randomly oriented bladed and lath-shaped barite crystals. Coarse crystals of mica are locally present as well. The dolomitic outer zone (mostly dolomite II) contains quartz, small micas and hematite, all being of authigenic origin.

### **c) Barite concretions** (pl. 1, figs. 1–3; pl. 3, fig. 2, and pl. 4, figs. 1–3)

These concretions exceed 5mm in diameter and consist of randomly oriented, inclusion-pure, bladed and lath-shaped barite crystals. These crystals are surrounded by a thin (< 1 mm) rim of authigenic quartz, dolomite and micas. In some samples the barite crystals are surrounded by a hematite rim ( $\leq 3$ mm).

The barite crystals are lath-shaped, very coarse-crystalline (>1cm) and free of impurities (pl. 2, fig. 5). Remaining pore space is filled by dolomite (pl. 1, fig. 1). The barite crystals show prominent cleavage and locally undulose extinction (pl. 1, fig. 3). Quartz and dolomite replaced the barite crystals along cleavage planes and crystal boundaries.

Most barite does not show any visible CL, only a few samples showed dull blue CL colours. Dolomite displays red CL colours.

The rim is composed of fine-crystalline authigenic quartz and some dolomite. The grain size of the quartz increases toward the core of the concretions. At the rim-core boundary the barite crystals are replaced by quartz and dolomite (pl. 2, figs. 3 and 4).

Within the rim euhedral dolomite rhombs (dolomite II), micas and a few hematite crystals grew and replaced quartz.

Small barite relics within the rim are in optical continuity with the large barite crystals of the core, suggesting that barite was later replaced by quartz, dolomite and micas along the margin of the concretions. From these observations the following reaction series is suggested. Barite and dolomite I were the first phases, followed by quartz (replaced barite and dolomite I), dolomite II (dolomite rhombs, replacing quartz) and finally micas and hematite crystals formed, replacing all other phases.

These observations also indicate, that the small, barite-free concretions originally were also composed of barite, which during a later phase were replaced by quartz, dolomite, micas and hematite.

### **4.3 Mineral chemistry and cathodoluminescence microscopy**

Micas within the concretions show chemical compositions typical of muscovite-phengite. As these authigenic micas are small and not abundant, it was not possible to separate enough material for X-ray diffractometry. The micas of the concretions are characterized by significantly lower Na<sub>2</sub>O- and TiO<sub>2</sub> concentrations as compared to detrital micas of the karst sediment (see table 1).

The carbonate of the matrix of the karst sediment is composed of dolomite with FeO contents of about 1.5 wt.%. The dolomite rhombs of the matrix are lower in FeO (about 0.4 wt.%). The dolomites of the concretions display variable FeO contents of up to 2.1 wt.%. The MnO content of all dolomite types ranges from 0.1–0.3 wt.% (table 2).

In all five investigated samples the Sr content of the barite was below 1 wt.%.

	1	2	3	4	5	6	7	8
	$x=7$	$x=7$	$x=10$	$x=7$	$x=4$	$x=4$	$x=5$	$x=4$
SiO <sub>2</sub>	47,55	47,37	47,61	47,2	46,59	47,38	48,21	47,46
TiO <sub>2</sub>	0,01	0,02	0,01	0,6	0,53	0,	0,08	0,6
Al <sub>2</sub> O <sub>3</sub>	34,02	37,12	36,68	37,15	38,15	37,93	36,89	37,8
Cr <sub>2</sub> O <sub>3</sub>	0,02	<DL	0,01	<DL	0,01	<DL	<DL	0,04
FeO	0,8	0,53	0,48	1,06	0,72	0,98	1,44	0,81
MnO	0,01	0,02	0,01	<DL	0,02	<DL	0,01	0,01
MgO	1,12	1,12	0,95	0,71	0,65	0,83	1,63	0,58
CaO	0,1	0,03	0,04	0,03	0,04	0,02	0,03	0,04
Na <sub>2</sub> O	0,18	0,22	0,17	0,73	1,42	0,17	0,26	0,77
K <sub>2</sub> O	10,6	8,89	9,18	9,3	8,12	8,31	8,34	8,36
Total	94,41	95,32	95,14	96,84	96,25	96,72	96,89	96,47

**Table 1:** Chemical composition of micas in karst sediments and concretions (in wt.%):

1–3: authigenic micas in concretions

4–6: detrital micas of the karst sediment

7–8: detrital micas in siltstones near concretions

	1	2	3	4	5
	$x=6$	$x=6$	$x=6$	$x=6$	$x=7$
CaO	30,48	30,21	30,21	31,37	30,81
MgO	20,63	20,84	20,71	21,15	21,4
FeO	1,34	1,48	2,09	0,53	0,41
MnO	0,15	0,12	0,31	0,12	0,11
Total	52,60	52,65	53,32	53,17	52,73

**Table 2:** Chemical composition of dolomite:

1–2: dolomite of the matrix

3–4: dolomite near concretions    5: dolomite rhombs within concretions (dolomite II)

### 3.4 Barite nodules of the Tannheim Beds

Barite nodules from the Cretaceous (Late Aptian to Albian) Tannheim Beds of the Northern Calcareous Alps near Vils (Tyrol) have also been studied for comparative purpose. The Tannheim Beds reach a maximum thickness of

80–90 m and consist of grey pelagic marls (see TOLLMANN, 1976). Near Vils these marls contain barite nodules. These nodules are composed of fine-grained, radiating calcite and barite crystals with minor interstitial clay. The barite concretions are typically 5–10 cm in diameter and of spherical shape. Septarian cracks are present in



the center, filled by coarse-crystalline, inclusion-pure barite crystals and minor calcite (pl. 3, fig. 1). The nodules are similar to the barite nodules described from the Devonian of western Virginia (CLARK & MOSIER, 1989), from the Mississippian of Arkansas (ZIMMERMANN & AMSTUTZ, 1966) and from modern ocean-floor sediments (REVELLE & EMERY, 1951).

Although the barite nodules of the Tannheim Beds formed in a different environmental setting compared with the barite nodules of the karst sediments, this example shows that early diagenetic barite nodules are frequently composed of fine-grained, radial barite crystals.

#### 4. Discussion

Barite nodules in sediments are a typical diagenetic feature. Most barite nodules described in the literature are of early diagenetic origin, in most cases growth already began in unconsolidated sediments (BOGOCH et al., 1977, CARLSON & HOLDEN, 1977, CLARK, 1985, CLARK & MOSIER, 1989, HEMINGWAY & VONDRA, 1992, NUELLE & SHELTON, 1986, PEPPER et al., 1985, WETZEL, 1970). In contrast, LAZNICKA (1976) suggests that barite nodules in Devonian (?)/Mississippian carbonaceous shales and argillaceous dolomitic limestones in the Mackenzie Mountains, Canada, formed during late diagenesis postdating the formation of carbonate concretions, dolomitization, and an early phase of fracturing.

Most of the diagenetically formed barite nodules are composed of grey, fine-grained, commonly radiating barite with some interstitial clay. In some nodules calcite is present in high amounts (BOGOCH et al., 1977).

In the pelagic environment barite forms below the sediment - water interface at the redox boundary between deeper anoxic waters and overlying oxygenated waters of the dysaerobic zone (CLARK, 1985, CLARK & MOSIER, 1989, PEPPER et al., 1985).

Although barite is common as cement and in concretionary form in red bed sediments, little is

known about the geochemical conditions of barite nodule formation. The occurrence of barite in red coloured karst sediments indicates, that the barite nodules grew in an oxygenated environment under conditions different from that in the pelagic environment.

The deformation of laminae in the enclosing shales and siltstones around the nodules indicates that the barite nodules grew within unconsolidated sediment. The sulphur isotope composition of four barite samples yielded  $\delta^{34}\text{S}$  values ranging from +7.5 to +8.8‰ (SCHROLL & PAK, 1980), suggesting that the sulphate is derived from Permian seawater or the dissolution of marine Permian evaporites. SCHROLL & PAK (1980) pointed out that the sulphur isotopic composition does not allow a genetic interpretation of the barite formation.

The growth rates of diagenetically formed spherical concretions from flowing and non-flowing pore waters have been calculated by BERNER (1968, 1971, 1980). He pointed out that concretions of calcite, siderite and pyrite of a few centimeters in size may form within a very short time span of about 12,000 years, and that flow rates are relatively unimportant on the growth rates.

It is assumed that the barite nodules in the karst sediments formed by similar growth rates during early diagenetic precipitation from Barich porewaters, and that they originally were composed of fine-grained barite with radial internal structures and interstitial clay.

During burial the barite nodules experienced recrystallization and a change in mineralogical composition. Recrystallization of dolomite and of the fine-grained barite resulted in larger, randomly oriented, lath-shaped barite and blocky dolomite crystals. Petrographic observations show that barite and dolomite I were later replaced by quartz, dolomite II, newly formed micas (phengite-muscovite) and hematite. During early Alpine metamorphism (HOSCHEK et al. 1980, COLINS et al. 1980, SCHRAMM, 1980, KRALLIK et al. 1987) these minerals formed within the small concretions as well as along the rim of the larger barite concretions. Replacement of

barite and dolomite I occurred from the rim toward the center of the nodules and along cleavage plains and crystal boundaries of the large barite crystals. The unusual structure and composition of the barite nodules of the karst sediments from the Kitzbühler Horn compared to the early diagenetic barite nodules was caused by this late diagenetic and metamorphic overprint.

The source of the Ba remains an unsolved problem. Ba-rich hydrothermal fluids in connection with submarine volcanism as well as biogeochemical processes can be ruled out. For similar barite mineralizations hosted in the Lower Devonian Schwaz Dolomite near Brixlegg FRIMMEL (1989) recently suggested an epigenetic origin from hydrothermal Ba-rich solutions derived from older rocks during Variscan metamorphism. It is suggested that the Ba of the barite mineralizations and nodules near the Kitzbühler Horn was remobilized from older rocks (e.g. Wildschönauer Schiefer) or derived from the weathering of Ba-rich feldspars.

## Acknowledgements

The author wishes to thank Dr. Richard Tessadri (Innsbruck) for electron microprobe analysis and Mag. Dr. Christoph Spötl (Reston-Innsbruck) for constructive comments, suggestions and discussion during preparation of the manuscript.

## References

- BERNER, R.A. (1968): Rate of concretion growth. – *Geochim. Cosmochim. Acta*, **32**, 477–483.
- BERNER, R.A. (1971): *Principles of Chemical Sedimentology*. – McGraw-Hill, New York, 240 pp.
- BERNER, R.A. (1980): *Early Diagenesis. A Theoretical Approach*. – Princeton University Press, Princeton, N.J., 241 pp.
- BOGOCH, R., BUCHBINDER, B. & NIELSEN, H. (1987): Petrography, geochemistry, and evolution of barite concretions in Eocene pelagic chalks from Israel. – *Jour. Sed. Petrol.*, **57**, 3, 522–529.
- CARLSON, E.H. & HOLDEN, W.F. (1977): Barite concretions from the Cleveland Shale. – *Geol. Soc. Am., Abstr. Programs*, **9**, 5, 580–581.
- CLARK, S.H.B. (1985): Diagenetic barite nodules in Ordovician and Devonian shales of the Appalachian Basin. – *Geol. Soc. Am., Abstr. Programs*, **17**, 7, p. 548.
- CLARK, S.H.B. & MOSIER, E.L. (1989): Barite nodules in Devonian shale and mudstone of Western Virginia. – *U.S. Geol. Surv. Bull.*, **1880**, 1–30.
- COLINS, E., HOSCHEK, G. & MOSTLER, H. (1980): Geologische Entwicklung und Metamorphose im Westabschnitt der Nördlichen Grauwackenzone unter besonderer Berücksichtigung der Metabasite. – *Mitt. österr. geol. Ges.*, **71/72**, 343–378.
- EMANUILIDIS, G. & MOSTLER, H. (1970): Zur Geologie des Kitzbühler Horns und seiner Umgebung mit einem Beitrag über die Barytvererzung des Spielbergdolomits. – *Festbd. Geol. Inst., 300-Jahr-Feier Univ. Innsbruck*, 547–569.
- FRIMMEL, H. (1989): Einsatzmöglichkeiten der Strontium-Methode in der Lagerstättengeologie am Beispiel der Barytlagerstätte Kogel/Brixlegg (Tirol). – *Arch. f. Lagerst.forsch. Geol. B.-A.*, **11**, 127–146.
- HAAGE, R. & KRUMBIEGEL, G. (1968): Über die Barytvorkommen im Tertiär des Geiseltales. – *Geologie*, **17**, 10, 1195–1207.
- HAM, W.E. & MERRITT, C.A. (1944): Barite in Oklahoma. – *Oklahoma Geol. Surv., Circ.*, **23**, 42 pp.
- HEMINGWAY, S.J. & VONDRA, C.F. (1992): The origin of nodules in the Lower Cretaceous Clover Formation, Bighorn Basin, Wyoming. – *Geol. Soc. Am., Abstr. Programs*, **24**, 4, p. 20.

- HOLDEN, W.F. & CARLSON, E.H. (1979): Barite concretions from the Cleveland Shale in Northern-Central Ohio. – *Ohio J. Sci.*, **79**, 5, 227–232.
- HOSCHEK, G., KIRCHNER, E. Ch., MOSTLER, H. & SCHRAMM, J.-M. (1980): Metamorphism in the Austroalpine Units between Innsbruck and Salzburg (Austria) – A Synopsis. – *Mitt. österr. geol. Ges.*, **71/72**, 335–341.
- KEYSER, A.W. (1966): Some indications of arid climate during the deposition of the Beaufort Series. – *Annals Geol. Surv. S. Afr.*, **5**, 77–79.
- KRAINER, K. & STINGL, V. (1986): Alluviale Schuttfächersedimente im Ostalpinen Perm am Beispiel der Präbichlschichten an der Typuslokalität bei Eisenerz/Steiermark (Österreich). – *Mitt. österr. geol. Ges.*, **78**, 231–249.
- KRALIK, M., KRUMM, H. & SCHRAMM, J.-M. (1987): Low Grade and Very Low Grade Metamorphism in the Northern Calcareous Alps and in the Greywacke Zone: Illite-Crystallinity Data and Isotopic Ages. – In: FLÜGEL, H.W. & FAUPL, P. (eds.), *Geodynamics of the Eastern Alps*, 164–178, F. Deuticke, Vienna.
- LAZNICKA, P. (1976): Barite nodules of possibly late diagenetic origin from Twitya River area, Mackenzie Mountains, Northwest Territories. – *Can. J. Earth Sci.*, **13**, 1446–1455.
- LEITMEIER, H. (1936): Die Barytvorkommen am Kitzbüheler Horn. – *Zeitschr. Kristallogr., Abt. B, Mineral. Petrogr. Mitt.*, N.F., **47**, 1, 1–25.
- MAVRIDIS, A. & MOSTLER, H. Zur Geologie der Umgebung des Spielberghorns mit einem Beitrag über die Magnesitvererzung (Nördliche Grauwackenzone; Tirol, Salzburg). – *Festbd. Geol. Inst., 300-Jahr-Feier Univ. Innsbruck*, 523–546.
- MOSTLER, H. (1970): Zur Baryt-Vererzung des Kitzbühler Horns und seiner Umgebung (Tirol). – *Arch. Lagerstättenforsch. Ostalpen*, **11**, 101–112.
- MOSTLER, H. (1984): An jungpaläozoischen Karst gebundene Vererzungen mit einem Beitrag zur Genese der Siderite des Steirischen Erzberges. – *Geol. Paläont. Mitt. Innsbruck*, **13**, 4, 97–111.
- MOSTLER, H., KRAINER, K. & STINGL, V. (1982): Untersuchung der Schwespatvorkommen Tirols im Hinblick auf eine wirtschaftliche Nutzung. – *Unpubl. Report*, 74 p.
- NUELLE, L.M. & SHELTON, K.L. (1986): Geologic and geochemical evidence of possible bedded barite deposits in Devonian Rocks of the Valley and Ridge Province, Appalachian Mountains. – *Economic Geology*, **81**, 1408–1430.
- PEPPER, J.F., CLARK, S.H.B. & DE WITT, W. (1985): Nodules of diagenetic barite in Upper Devonian shales of Western New York. – *U.S. Geol. Surv. Bull.*, **1653**, 1–11.
- REVELLE, R. & EMERY, K.O. (1951): Barite concretions from the ocean floor. – *Bull. Geol. Soc. Am.*, **62**, 707–724.
- SCHÖNLAUB, H.P., KLEIN, P., MAGARITZ, M., RANTITSCH, G. & SCHARBERT, G. (1991): Lower Carboniferous Paleokarst in the Carnic Alps (Austria, Italy). – *Facies*, **25**, 91–118.
- SCHRAMM, J.-M. (1977): Über die Verbreitung epi- und anchimetamorpher Sedimentgesteine in der Grauwackenzone und in den Nördlichen Kalkalpen (Österreich) – ein Zwischenbericht. – *Geol. Paläont. Mitt. Innsbruck*, **7**, 2, 3–20.
- SCHRAMM, J.-M. (1978): Anchimetamorphes Permoskyth an der Basis des Kaisergebirges (Südrand der Nördlichen Kalkalpen zwischen Wörgl und St. Johann in Tirol, Österreich). – *Geol. Paläont. Mitt. Innsbruck*, **8** (Festschrift W. Heiße), 101–111.
- SCHRAMM, J.-M. (1980): Bemerkungen zum Metamorphosegeschehen in klastischen Sedimentgesteinen im Salzburger Abschnitt der Grauwackenzone und der Nördlichen Kalkalpen. – *Mitt. österr. geol. Ges.*, **71/72**, 379–384.
- SCHROLL, E. & PAK, E. (1980): Schwefelisotopenzusammensetzung von Baryten aus den Ost- und Südalpen. – *Tschermaks Min. Petr. Mitt.*, **27**, 79–91.
- SHEAD, A.C. (1923): Notes on barite in Oklahoma with chemical analyses of barite rosettes. – *Proc. Oklahoma Acad. Sci.*, **3**, 102–106.
- STINGL, V. (1983): Ein Beitrag zur Fazies der Prebichlschichten zwischen St. Johann i.T. und Leogang (Tirol/Salzburg). – *Geol. Paläont. Mitt. Innsbruck*, **12**, 10, 207–233.
- TARR, W.A. (1933): The origin of sand barites of the Lower Permian of Oklahoma. – *Amer. Mineral.*, **18**, 260–272.
- TOLLMANN, A. (1976): Analyse des klassischen nordalpinen Mesozoikums. – *Monographie der Nördlichen Kalkalpen, Teil II*, 580 pp., F. Deuticke, Wien.
- VAN EEDEN, O.R. (1937): The Geology of the country around Bethlehem and Kestell, with special reference to oil indications. – *S. Afr. Geol. Surv., Memoir* **33**.

VOHRZYKA, K. (1968): Die Erzlagerstätten von Nordtirol und ihr Verhältnis zur alpinen Tektonik. – Jb. Geol. B.-A., **111**, 3-38.

WETZEL, W. (1970): Die Erscheinungsformen des Barytes in jungkretazischen und ältertiären Sedimenten. – N. Jahrb. Mineral., Mh., **1**, 25–29.

ZIMMERMANN, R.A. & AMSTUTZ, G.C. (1964): Small scale sedimentary features in the Arkansas Barite

District. – In: AMSTUTZ, G.C. (Ed.), *Sedimentology and Ore Genesis*, 157–163, Elsevier, Amsterdam.

*Author's address:*

*Univ.-Doz. Dr. Karl Krainer, Institut für Geologie und Paläontologie, Innrain 52, A-6020 Innsbruck, Austria.*

Manuscript submitted: October 17, 1994

## Plate 1

- Fig. 1: Barite nodule composed of coarse, lath-shaped, randomly oriented barite crystals. Pore space between the barite crystals is filled by dolomite (D). The barite nodule is embedded in silty karst sediments and surrounded by a thin rim of fine-grained quartz and dolomite. Crossed nicols, scale bar = 2 mm.
- Figs. 2, 3: Barite nodule embedded in silty karst sediments. Scale bar = 1 mm, 2 = plane light, 3 = crossed nicols.
- Fig. 4: Karst sediment composed of a dark, fine-grained groundmass and recrystallized, mostly euhedral dolomite rhombs. Plane light, scale bar = 0.3 mm.
- Fig. 5: Red siltstone (karst sediment) composed of anhedral to euhedral dolomite grains, detrital micas, angular quartz fragments and a hematite-pigmented, fine-grained groundmass. Plane light, scale bar = 0.4 mm.



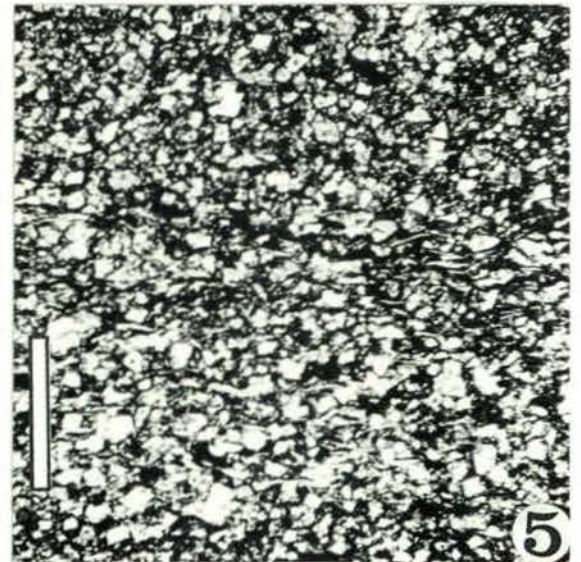
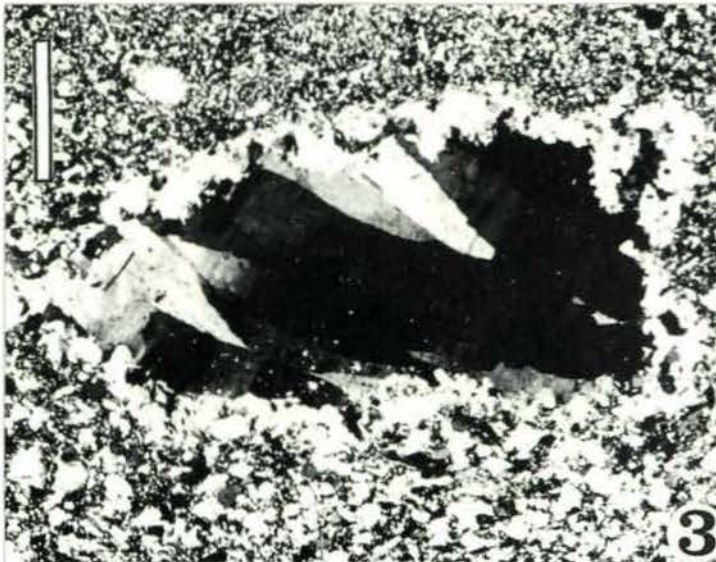
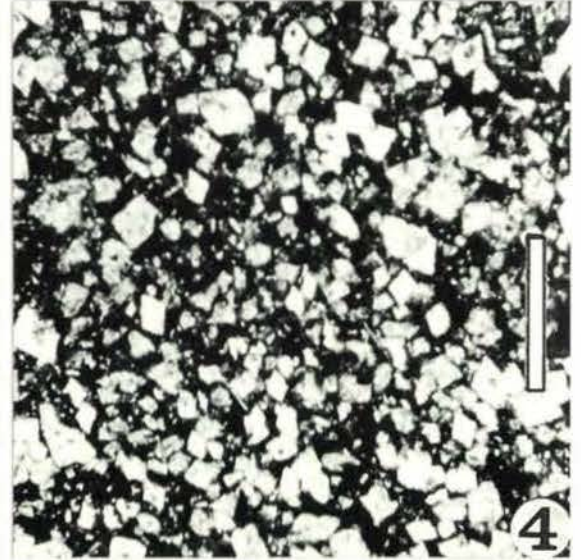
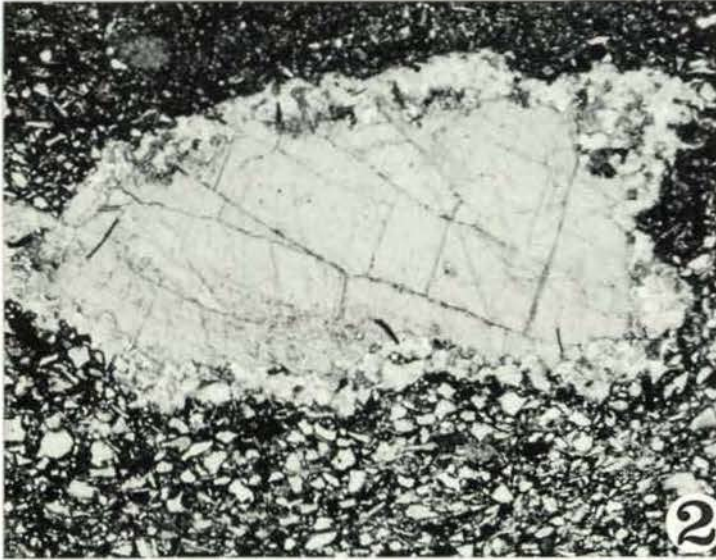
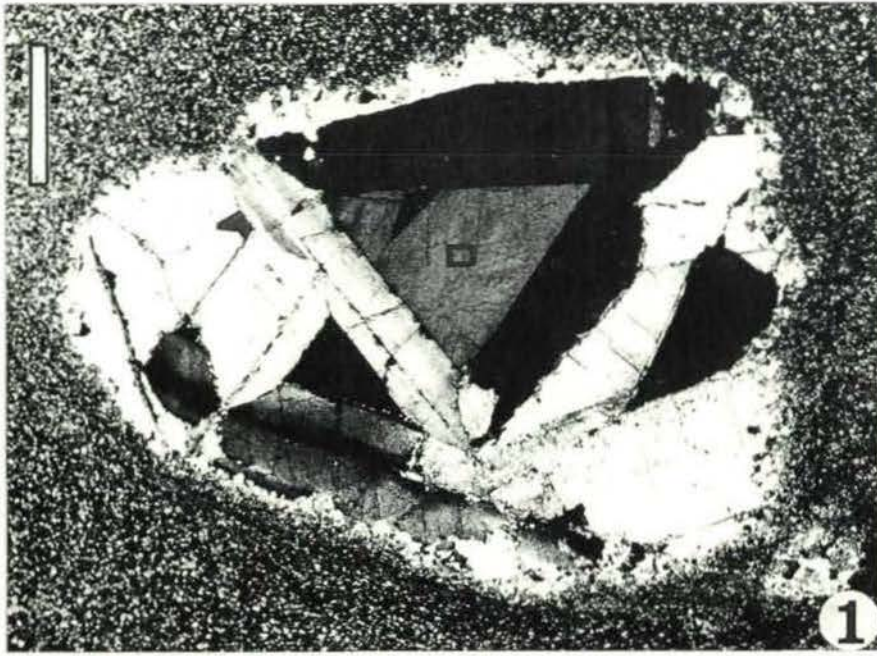


## Plate 2

- Fig. 1: Small concretion in fine-grained, red-colored karst sediment. The concretion is formed of authigenic micas, quartz and dolomite. Crossed nicols, scale bar 0.5 mm.
- Fig. 2: Small concretion composed mainly of dolomite (D) and some authigenic micas (M). The larger concretions consist of coarse barite crystals, surrounded and replaced by authigenic quartz, dolomite and micas. Crossed nicols, scale bar 1 mm.
- Fig. 3: Thin section photograph of the outer zone of a barite nodule. Along the margin the large barite crystals are replaced by fine-grained authigenic quartz, dolomite and micas. Dark, fine-grained karst sediment is visible on top of the photograph. Crossed nicols, scale bar 0.4 mm.
- Fig. 4: Detail of a barite nodule composed of large barite crystals which are replaced by fine-grained, authigenic quartz, dolomite and micas along the margin. Crossed nicols, scale bar 1 mm.
- Fig. 5: Detail from the central part of a barite nodule, composed of large, randomly oriented, lath-shaped barite crystals. Crossed nicols, scale bar 3 mm.



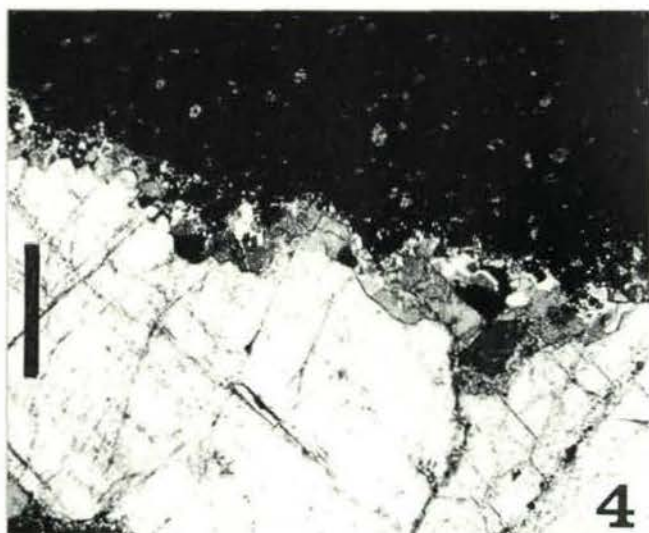
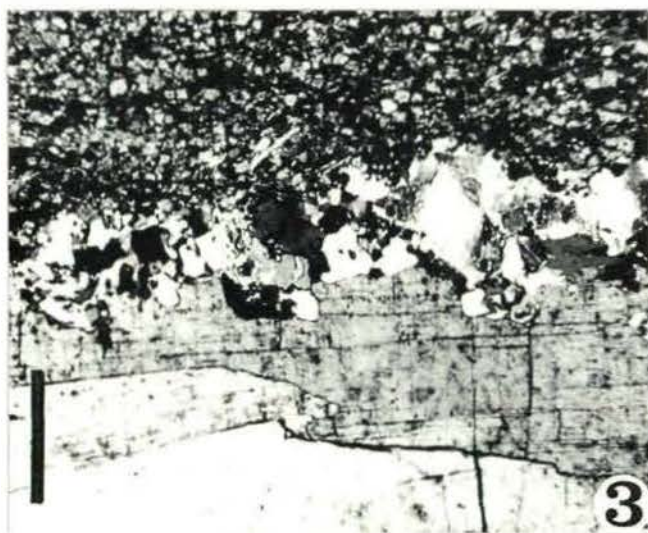
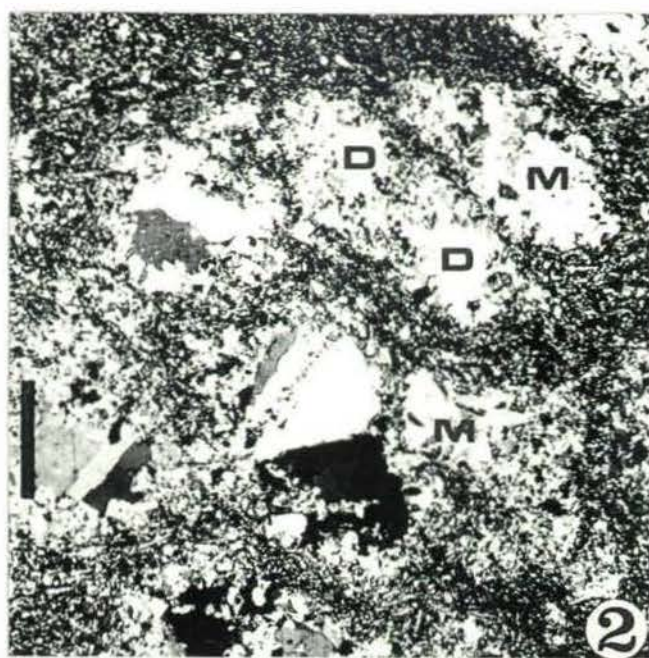
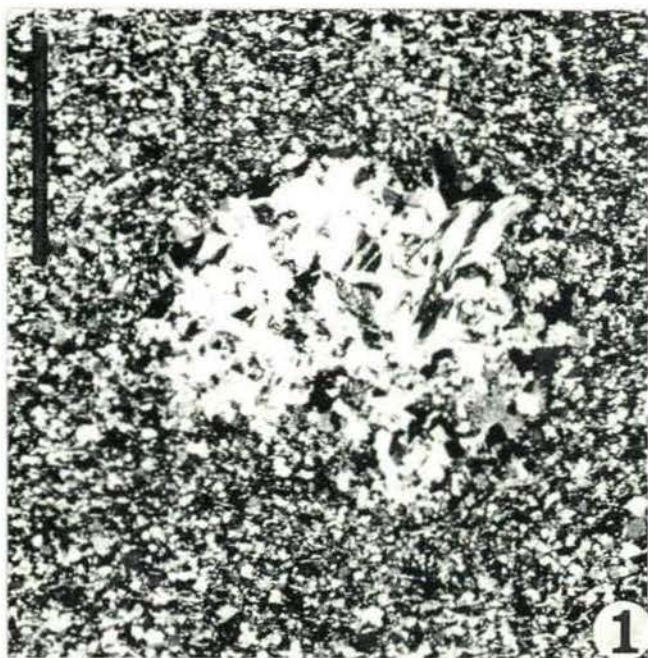


### Plate 3

- Fig. 1: Thin section photograph of a barite nodule (central part) from the Tannheim Beds. The nodule is composed of fine-grained barite and calcite crystals. Septarian cracks are filled by coarse barite. Crossed nicols, scale bar 2 mm.
- Fig. 2: Barite nodule in fine-grained karst sediment. The nodule is formed of coarse barite crystals and a thin rim of fine-grained authigenic quartz, dolomite and micas. Crossed nicols, scale bar 2 mm.
- Fig. 3: Fine-grained, laminated karst sediment containing a few, anhedral to euhedral dolomite rhombs. Plane light, scale bar 1 mm.
- Fig. 4: Concretion composed of radially arranged authigenic micas, dolomite and quartz. Plane light, scale bar 0.4 mm.
- Fig. 5: Karst sediment in form of fine grained sandstone composed of angular quartz and detrital micas in a dolomitic and clay-rich, hematite-pigmented groundmass. Plane light, scale bar 0.5 mm.



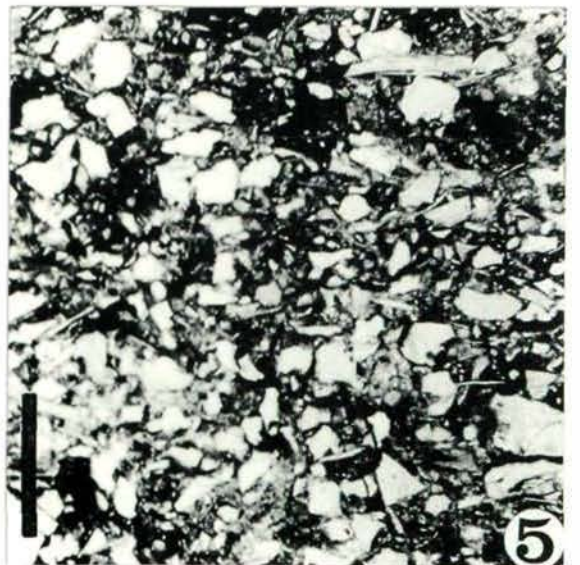
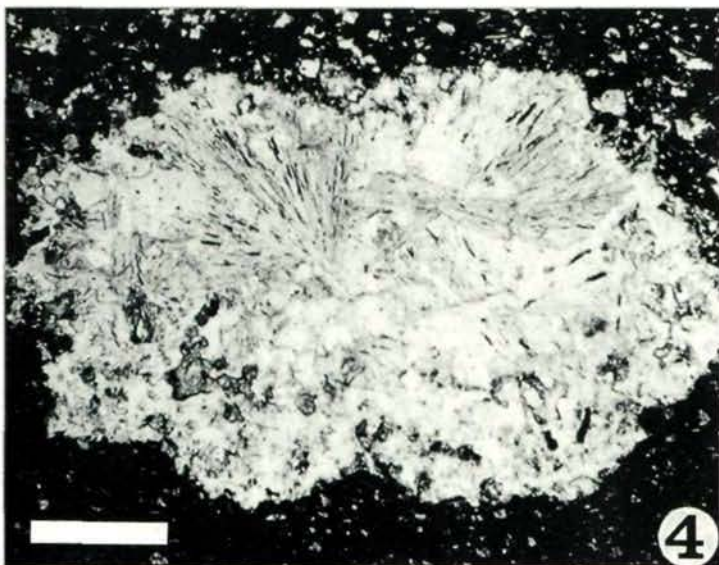
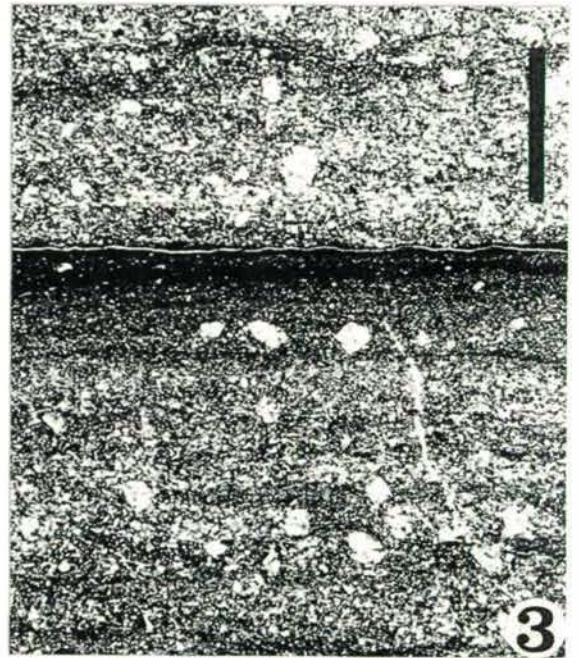
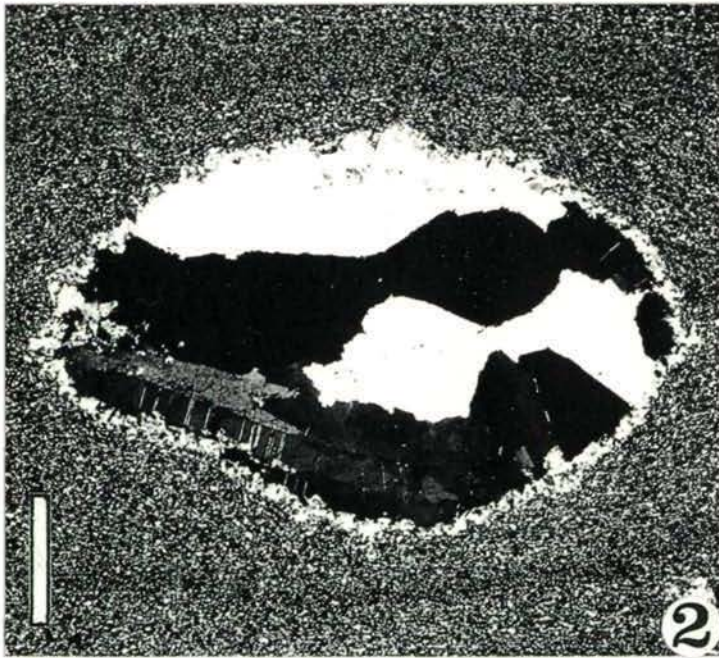
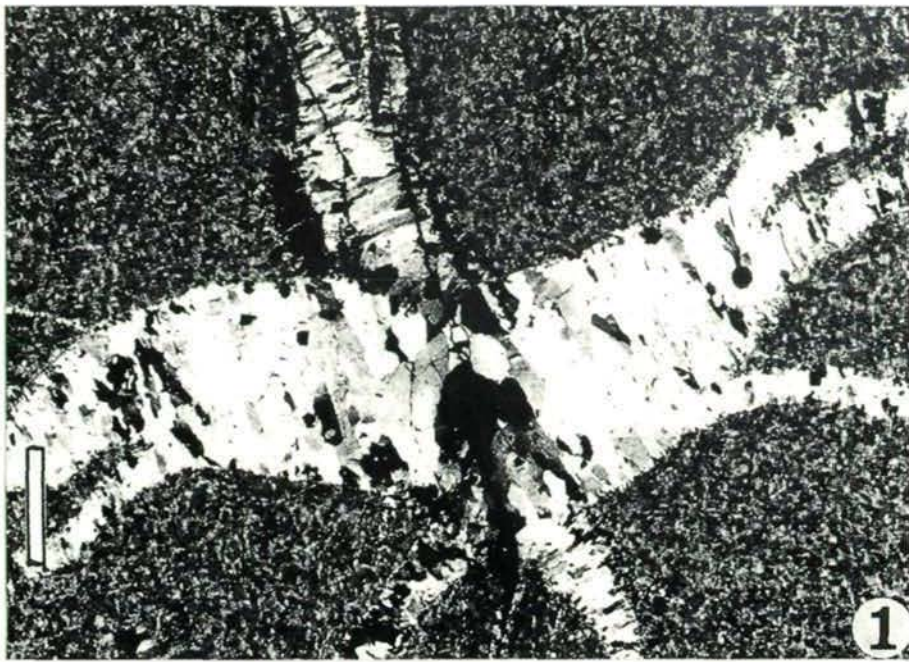


## Plate 4

Figs. 1, 2: Elongated barite nodule composed of coarse barite crystals which are surrounded by a thin rim of fine-grained authigenic quartz, dolomite and micas. Fig 1 under plane light, fig. 2 under crossed nicols, scale bar 1.2 mm.

Fig. 3: Elongated barite nodule formed of large barite crystals, surrounded by fine-grained karst sediment. Crossed nicols, scale bar 3 mm.



